Energy 171 (2019) 556–565

Contents lists available at ScienceDirect

Energy

journal homepage: www.elsevier.com/locate/energy

Unbalance evaluation of a scaled wind turbine under different rotational regimes via detrended fluctuation analysis of vibration signals combined with pattern recognition techniques

Francisco Erivan de Abreu Melo Junior [a], Elineudo Pinho de Moura [b, *], Paulo Alexandre Costa Rocha [a], Carla Freitas de Andrade [a]

[a] Departamento de Engenharia Mecânica, Universidade Federal do Ceará, 60455-760, Fortaleza, CE, Brazil
[b] Departamento de Engenharia Metalúrgica e de Materiais, Universidade Federal do Ceará, 60455-760, Fortaleza, CE, Brazil

ARTICLE INFO

Article history:
Received 10 August 2018
Received in revised form
19 December 2018
Accepted 9 January 2019
Available online 11 January 2019

Keywords:
Machine learning
Signal processing
Fault detection
Condition monitoring
Non-stationary vibration
Condition based maintenance

ABSTRACT

This work aims to propose a different approach to evaluate the operating conditions of a scaled wind turbine through vibration analysis. The turbine blades were built based on the NREL S809 profile and a 40-cm diameter, while the design blade tip speed ratio (λ) is equal to 7. Masses weighing 0.5, 1.0, and 1.5 g were added to the tip of one or two blades in a varying sequence with the intent of simulating potential problems and producing several scenarios from simple imbalances to severe rotor vibration levels to be compared to the control condition where the three blades and the system were balanced. The signals were processed and classified by a combination of detrended fluctuation analysis with Karhunen-Loève Transform, Gaussian discriminator, and Artificial Neural Network, which are pattern recognition techniques with supervised learning. Good results were achieved by employing the above cited recognition techniques as more than 95% of normal and imbalanced cases were correctly classified. In a general way, it was also possible to identify different levels of blade imbalance, thus proving that the present approach may be an excellent predictive maintenance tool for vibration monitoring of wind turbines.

1. Introduction

The increasing global demand for energy has caused several environmental problems due to high atmospheric emissions of CO_2. Global warming is a great concern and efforts are being done made to reduce CO_2 emissions. So there is growing interest in alternative energy sources, and among them wind energy is considered one of the cleanest, most efficient, and least environmentally harmful.

Wind turbines are devices exposed to weathering throughout the day. Many wind farms have been established in coastal regions where greater aggression against metallic materials occurs, reducing the equipment's lifetime. In those regions, wind speeds vary continuously during the day, which may cause undesired vibration and fatigue failure.

One of the most critical parts of a wind turbine is its rotor, which is responsible for converting the wind energy. The manufacturing cost of wind turbine blades can represent over 20% of the turbine's production cost [1]. Its blades can be damaged by mechanisms such as atmospheric corrosion and erosion [2,3], fatigue [4], unbalancing by accumulation of dirt, ice [3,5], and insect contamination [3,5,6], lightning strikes [7], and so on. These occurrences contribute to higher turbulence intensity levels at the blades' surface and can reduce the annual energy production of a wind turbine by up to 25%. Furthermore, failure of a blade can damage other blades or wind turbines or cause harm to people nearby [8]. Therefore, it is advisable to apply condition-monitoring techniques to wind turbine blades to detect the damage before a blade fails catastrophically.

Vibration-based monitoring techniques are widely adopted for machines, and new approaches based on the decomposition of the vibration signals have been developed for fault diagnosis in wind turbines. Abouhnik and Albarbar [9] stated that the nature of the vibration signals of a wind turbine is complex due to the existence of several sources with different frequencies and developed a novel approach called Empirically Decomposed Feature Intensity Level

* Corresponding author.
E-mail address: elineudo@ufc.br (E.P. de Moura).

https://doi.org/10.1016/j.energy.2019.01.042
0360-5442/

Acronyms list

ANN	Artificial Neural Network
Cp	Performance coefficient
DFA	Detrended Fluctuation Analysis
EDFIL	Empirically Decomposed Feature Intensity Level
HAWT	Horizontal-axis wind turbine
h-NLPCA	hierarchical nonlinear Principal Component Analysis
KLT	Karhunen-Loève Transform
NREL	National Renewable Energy Laboratory
PCA	Principal Component Analysis
TSR	Tip Speed Ratio

Symbols list

u	Original time series
u	Average of the original series
y_j	Integrated time series
N	Time series length
$\tilde{y}_j$	Local trend of the series
$F(\tau)$	Fluctuation function
τ	Window sizes of the time series
$\mathbf{x}$	input vector
$\mathbf{m}_i$	average vector associated to class i
$\mathbf{m}_k$	mean vector of class k
$\mathbf{m}$	overall mean vector
$\mathbf{S}_i$	covariance matrix associated to class i
$\boldsymbol{S_B}$	between-class covariance matrix
$\boldsymbol{S_w}$	within-class covariance matrix
N_C	Number of classes
N_k	Number of vectors in class k
$\mathbf{X}$	Matrix of training vectors
$\mathbf{\Lambda}$	Matrix of variances of the transformed features (eigenvalues of $\mathbf{S}_W$)
$\mathbf{U}$	Eigenvectors of $\mathbf{S}_W$
$\mathbf{V}$	Eigenvectors of $\mathbf{S}_B$
T	Matrix transpose
N	Size of the dataset
λ	Tip speed ratio

(EDFIL), which was successfully employed to analyze the vibration signals of flaw of different severities caused by four different lengths of cracks introduced in a wind turbine blade to simulate real conditions. In Ref. [10], a new method based on the local mean decomposition was applied to identify failures from the turbine's gearbox. These new approaches were efficient in performing fault diagnosis in machines with nonlinear vibration signals, while the traditional time-frequency analysis techniques did not present satisfactory results and are not recommended for these situations.

Using pattern recognition techniques, nonlinear vibration signals can be evaluated, allowing a better understanding of the vibration behavior produced by flaws in wind turbine blades. In Ref. [11], vibration analysis and pattern recognition techniques were used to identify and classify six different blade fault conditions, which simulated bending, cracking, erosion, hub-blade loose contact, pitch angle twist, and the control condition. The features of the vibration signals were extracted using traditional vibration analysis techniques. For the feature selection, a J48 decision tree algorithm was chosen and the feature classification was performed using best-first tree and functional-trees algorithms, which reached classification accuracies of 85.33 and 91.67%, respectively. In Ref. [12], hierarchical nonlinear Principal Component Analysis (h-NLPCA) was used as a pattern recognition technique to measure strains embedded into the wind turbine blades from data acquired in real time by two different fiber optic sensor technologies. When using the index Q, which is a measure of the difference between a sample and its projection in the main components retained by the Principal Component Analysis (PCA) model, all abnormalities and nonlinearities could be detected during the classification, making it possible to avoid premature failure of the structure. One of the main drawbacks of h-NLPCA is the large computational cost.

Wind turbines have many sources of vibration, such as gears, bearings, shafts, generator, blades, and others, making vibration analysis complex and difficult to study. The use of detrended fluctuation analysis (DFA) [13] for processing non-stationary vibration signals combined with pattern recognition techniques proved to be effective in fault diagnosis of bearings [14]. Several combinations of loadings and operation frequencies were tested. In the processing phase, the combination of DFA with PCA presented satisfactory results, with above 80% of classifications being correct. Nevertheless, with the use of Neural Networks, a classification technique that applies supervised learning, the results were superior, reaching a correct classification rate of almost 100% in the training stage and above 89% in the tests. In Ref. [15], a similar approach was applied to detect different imbalance levels of a scaled wind turbine at a constant speed of 900 rpm and to evaluate the performance of DFA combined with three pattern recognition techniques, namely Artificial Neural Network (ANN), Karhunen-Loève Transform (KLT), and Gaussian discriminator, to classify data from vibration signals. Among the supervised training classification techniques, an average success rate above 98% was reached by all the classifiers, showing that these techniques are able to process and classify nonlinear vibration signals generated by unbalances of scaled wind turbine blades.

To deepen the present analysis, this study aims to evaluate the effectiveness of this approach in the monitoring of the working conditions of a scaled wind turbine. To perform this, a wide range of rotation velocities were tested, simulating possible failures by adding masses to the blades to induce unbalances and generate the corresponding vibration signals. Applying the DFA to process these signals and pattern recognition techniques to classify them, the approach sought to identify and classify different failure levels, which may be an important tool to monitor the operational conditions of wind turbine blades.

2. Experimental setup

In this work, a scaled horizontal-axis wind turbine (HAWT) was built for testing in a wind tunnel. The blades were built based on the NREL S809 profile and designed by in-house software [16], whose design methodology was taken from Ref. [17], to calculate blade parameters such as the chord and twist distributions. The chord and twist distributions of the blades used in this work were introduced in Ref. [15]. To guarantee the balancing of the blades and negligible roughness, 3D printing was used to manufacture the set of three blades, each 0.20 m in length with a mass of 15 g and design a tip speed ratio (TSR) equal to 7. During the tests, to maintain the TSR at its designed value, whenever the rotor speed was changed, the wind tunnel speed was set in a proportional way to keep the TSR equal to 7.

The experiments were carried out on a bench composed of a torque transducer, an electric motor, a wind turbine shaft, and the three blades, as shown in Fig. 1. This bench is located in an open circuit subsonic wind tunnel, 6.5 m long, powered by a 1.49-kW (2-

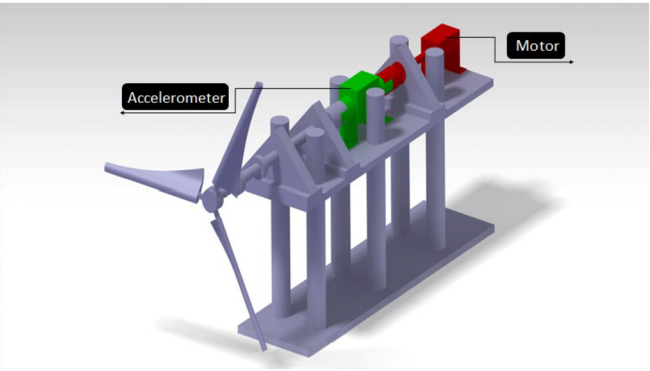

Fig. 1. Scaled wind turbine and measurement apparatus for a wind tunnel test.

hP) exhauster and a test section of 0.5 × 0.5 m that has a blockage ratio of 50.77% and a blockage factor of 0.84. The turbulence level at the test section is less than 2%. The existence of the motor is necessary for two reasons. In a first hypothesis (absence of the motor), if the turbine were to rotate freely, the generated power ($P = wT$) would be zero, because there would be no useful torque on the shaft. Secondly, torque is measured on the rotating shaft. This implies that the useful aerodynamic torque is continuously measured and used together with the spin value to obtain the aerodynamic power of the turbine. It is the presence of the motor that makes it possible to obtain and measure the useful torque produced by the turbine in the wind tunnel. In addition, it adjusts the rotation of the turbine in the wind tunnel, keeping the experiment under controlled conditions.

The objective of this work is to apply vibration analysis and pattern recognition techniques to identify different unbalancing levels in a scaled wind turbine, independently of its rotational speed. In practice, even with an optimum velocity defined by the project, the rotational speed of a wind turbine varies according to the wind speed, so in this work, rotations of 900, 1200 and 1500 rpm were applied to the rotor, covering a wide range of the scaled wind turbine operation. Therefore, the collected vibration signals were pre-processed by the DFA and the generated vectors were classified by the three pattern recognition techniques with supervised learning, namely the ANN, KLT, and Gaussian discriminator.

Blades were unbalanced using three different masses. A control condition with no additional mass was also used to simulate normal operation. This permitted seven working conditions to be reproduced:

1) In classes 1 to 3, masses weighing 0.5, 1, and 1.5 g were added at the tip of only one blade, respectively, representing a real situation of turbine operation where the damage can be caused by effects such as corrosion, accumulation of dirt and ice on a blade, and/or any attached object.
2) Classes 4 to 6 reproduce the possibility of a broken blade or excessive weight loss of a blade. To simulate this condition, masses of 0.5, 1, and 1.5 g were added at the tips of two blades, respectively, thus creating a severe imbalance at the rotor.
3) Finally, in Class 7, called the balanced system, all three blades had the same weight, which reproduced the normal condition of operation. In order to assess the balance of the system composed of the shaft and balanced blades, another set of signals was acquired using only the shaft in motion (without blades).

The vibration measuring system consisted of a Bruel & Kjaer piezoelectric accelerometer (model 4381 V), which captured the signals and sent them to a Bruel & Kjaer amplifier (model 2692). For band filtering, 1.0 Hz (high) and 100 Hz (low) were chosen as limits since the turbine rotational frequencies varied from 15 to 25 Hz. To record the generated signals, a Tektronix oscilloscope (model 1062 TBS) was used. Each signal was composed of 500 data points acquired at a sampling rate of 250 Hz (250 samples/s) according to the Nyquist sampling theorem, which corresponds to a time series of just 2 s duration. Although wind turbines do not operate in steady state conditions or uniform regimes, over short time scales it is possible to consider a quasi-steady state. For each unbalancing condition, 50 vibration signals were captured and a dataset of 400 vibration signals was obtained for each rotor speed, giving 1200 vibration signals in total.

3. Detrended fluctuation analysis

DFA [13] aims to identify long-range correlations in time series. With DFA, a simple quantitative parameter can be determined to extract features and represent the correlation properties of a random signal. By doing so, the method eliminates systematic trends in the data caused by external effects and reduces unwanted noise captured during the experimental phase.

The method consists in initially obtaining a new integrated series:

$$y_j = \sum_{i=1}^{j} (u_i - u) \tag{1}$$

where u is the overall average of the original series

$$u = \frac{1}{N} \sum_{i=1}^{N} u_i \tag{2}$$

The integrated series is divided into intervals of size τ where a linear data fitting is performed and the corresponding detrended fluctuations, defined as the difference between the integrated series y_j and the local trend $\tilde{y}_j$, are evaluated. It is normal practice to choose non-overlapping intervals. However, since the series length N may not be a multiple of the interval size, a small part at the end of the profile is lost. To overcome this problem, the solution proposed by Ref. [18] using overlapping time windows is applied. Thus, for each interval I_k , the variance of the residuals is calculated as

$$f_k^2(\tau) = \frac{1}{\tau - 1} \sum_{i \in I_k} (y_i - \tilde{y}_i)^2 \tag{3}$$

Lastly, the covariance $F(\tau)$ is calculated by summing over all overlapping $N - \tau + 1$ windows of size τ.

$$F(\tau) = \frac{1}{N - \tau + 1} \sum_{k} f_k(\tau) \tag{4}$$

From the values of $\log_{10}(F(\tau))$, vectors whose components correspond to the average fluctuation associated with suitably chosen interval sizes can be defined. In this work, the values of τ for each window of the accumulated series are obtained by taking the integer part of the division of the series length by $2^{\frac{1}{4}}$, that is, from 5 to 250. Thus, each DFA vector generated from each vibration signal has 24 components and the corresponding τ values are 5, 6, 7, 8, 9, 11, 13, 16, 19, 22, 26, 31, 37, 44, 53, 63, 74, 88, 105, 125, 149, 177, 210, and 250 (see Fig. 2).

Initially, DFA was developed to distinguish between local patchiness and long-range correlations in DNA sequences [13], but

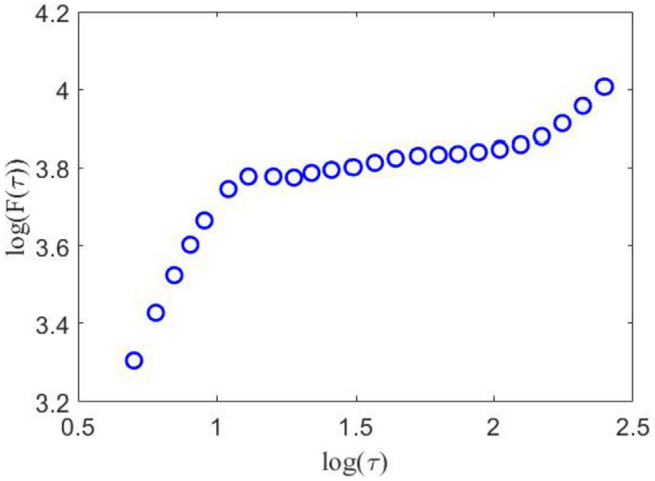

Fig. 2. Representative DFA curve generated with a vibration signal obtained from a balanced set of scaled wind turbine blades at a rotation speed of 1500 rpm for the present experiment.

it has been successfully applied in several studies of non-stationary time series such as gear fault diagnosis based on vibration signals [19], characterization of cast iron microstructures based on ultrasonic backscattered signals [20,21], and classification of welding defects from ultrasonic signals [22]. DFA has also been successfully applied in the processing stage of vibration signals generated by induced imbalances of a scaled wind turbine blade [15].

4. Supervised classification

The application of the DFA method to the captured vibration signals generates vectors which contain certain patterns that are not simple to classify. Pattern recognition techniques are used for this purpose and, in this work, three classification techniques, based on ANN, KLT, and Gaussian discriminator, are implemented. Similar approaches have been used for fault detection [23–25] and condition monitoring [15] specifically in wind turbines. A brief discussion of each technique is presented below.

4.1. Artificial neural networks

A basic neuron is commonly used to classify linearly separated data but in the case of complex and nonlinear wind turbine vibration signals, it is necessary to use a multilayer perceptron [26,27]. For this purpose, the network is composed of an input layer with 24 neurons which receive the data from DFA vectors, one hidden layer, and an output layer. The number of neurons of both the hidden and the output layer was changed according to the predefined number of classes. Each class is represented by one neuron in the output layer and the number of neurons in the hidden layer is calculated by the mean of the number of dimensions of the data and the number of classes to be used. Logistic sigmoid activation functions were used in all the neurons. The architecture and setup of the neural network are the same as were used by de Moura et al. [15].

The classification process is composed of two main steps. First, a set of input and output pairs is used to train the network and the synaptic weighting adjustment is performed by an error back-propagation learning algorithm that attempts to minimize the mean square error between the desired and actual outputs. The training is followed by the testing step, where the network is exposed to new data. In all cases, the input data (DFA vectors) were presented 1000 times; that is, the network was trained for 1000 epochs.

4.2. Gaussian classifier

The Gaussian function [28] also uses a supervised learning approach. It is a commonly applied method when data can be approximated to a multivariate normal distribution. In general, the p-dimensional Gaussian function for a given class i is given by:

$$p(\mathbf{x}|\omega_i) = \frac{1}{(2\pi)^{\frac{p}{2}}|\mathbf{S}_i|^{\frac{1}{2}}}\exp\left[-\frac{1}{2}(\mathbf{x}-\mathbf{m}_i)^{\mathrm{T}}\mathbf{S}_i^{-1}(\mathbf{x}-\mathbf{m}_i)\right] \tag{5}$$

where $\mathbf{S}_i$ is the covariance matrix associated with class i, $\mathbf{m}_i$ is the average vector also associated with class i, and $\mathbf{x}$ is an input vector. This function indicates the class to which a datum has a higher probability of belonging. When $\mathbf{x} = \mathbf{m}_i$, a maximum value of the Gaussian function is observed and the output of the function decreases with the increase of the distance between $\mathbf{x}$ and $\mathbf{m}_i$.

As a first step, a training set is used to calculate the mean vector and the covariance matrix of the Gaussian function for each class. The testing set is used to evaluate the performance of the Gaussian classifier in discriminating these vectors. They will be associated with the highest probability class obtained from the different Gaussian functions associated with each class.

4.3. Karhunen–Loève transformation

For the KLT [28], the input vectors $\mathbf{x}_i$ originated by DFA pass through an orthogonal transformation that produces a new set of uncorrelated variables. During this process, the training vectors are projected along the eigenvectors of the within-class covariance matrix defined by

$$\mathbf{S}_W = \frac{1}{N}\sum_{k=1}^{N_C}\sum_{i=1}^{N_k} y_{ik}(\mathbf{x}_i-\mathbf{m}_k)(\mathbf{x}_i-\mathbf{m}_k)^{\mathrm{T}} \tag{6}$$

where N is the number of samples of the dataset, N_C is the number of different classes, N_k is the number of vectors in class k, $\mathbf{m}_k$ is the mean vector of class k and T denotes the transpose vector. The element y_{ik} is equal to one if $\mathbf{x}_i$ belongs to class k, and zero otherwise.

A diagonal matrix built from the eigenvalues λ_j of $\mathbf{S}_W$ is used to rescale the resulting vectors. This operation can be written as

$$\mathbf{X}' = \mathbf{\Lambda}^{-\frac{1}{2}}\mathbf{U}^{\mathrm{T}}\mathbf{X} \tag{7}$$

where $\mathbf{X}$ is the matrix whose columns are the training vectors $\mathbf{x}_i$, $\mathbf{\Lambda} = \mathrm{diag}(\lambda_1, \lambda_2, \ldots)$ is the matrix of variances of the transformed features (eigenvalues of $\mathbf{S}_W$) and $\mathbf{U}$ is the matrix whose columns are the eigenvectors of $\mathbf{S}_W$.

Finally, to compress the class information, the resultant vectors are projected onto the eigenvectors of the between-class covariance matrix $\mathbf{S}_B$, calculated by:

$$\mathbf{S}_B = \sum_{k=1}^{N_C}\frac{N_k}{N}(\mathbf{m}_k-\mathbf{m})(\mathbf{m}_k-\mathbf{m})^{\mathrm{T}} \tag{8}$$

where $\mathbf{m}$ is the overall mean vector. The full transformation can be written as

$$\mathbf{X}'' = \mathbf{V}^{\mathrm{T}}\mathbf{\Lambda}^{-\frac{1}{2}}\mathbf{U}^{\mathrm{T}}\mathbf{X} \tag{9}$$

where $\mathbf{V}$ is the matrix whose columns are the eigenvectors of $\mathbf{S}_B$,

calculated from $\mathbf{X}'$.

The classification is performed by associating a vector $\mathbf{x}_i$ to the class whose mean vector remains closest to $\mathbf{x}_i$ within the dimensional transformed space.

5. Results and discussion

Firstly, the classification of the imbalance level was performed separately for data acquired at two rotation speeds (1200 and 1500 rpm).

For all classifiers, 80% of vectors yielded by DFA of vibration signals were randomly selected to define the training subset, while the testing subset was composed of the remaining 20% of vectors. The testing subset was used to evaluate the efficiency of classifiers in evaluating unknown data, that is, data not presented to the classifier during the training.

Tables 1 and 2 show the average success rate obtained by the three classifiers for training and testing vectors acquired at 1200 and 1500 rpm, respectively. These results are compared with ones presented in previous work for data acquired at 900 rpm [15]. Classifications were also performed for data obtained at all three of the abovementioned rotation speeds. Table 3 shows the average success rate of each pattern recognition algorithm for the classification of all 21 classes defined during the experimental planning, while Table 4 shows their average success rate in the classification of unbalance levels, regardless of rotation speed.

In all tables, the average performances were taken over 100 distinct choices of training and testing sets. This procedure ensures a good statistical significance.

Table 1 shows the classification results of the generated vectors at 1200 rpm. The numbers in the first column refer to the classes being studied. In the other columns, numbers indicate the percentage of vectors which were correctly classified and the values after "#" register average misclassification rates; for example, for class 1 of Gaussian classifier, #3:0.3 indicates that 0.3% of vectors belonging to class 1 were misclassified as belonging to class 3.

Table 1
Average performance of the classifiers used to classify the data in 7 classes. Average calculated over 100 sets of training and testing vectors. Classifiers applied to vectors built from vibration signals acquired at 1200 rpm.

Class	Gaussian		Karhunen-Loève		Neural Network	
	Training	Testing	Training	Testing	Training	Testing
1	100	95.50 #3:0.3 #4:2.3 #7:1.9	100	98.10 #4:1.6 #7:0.3	100	97.90 #4:0.4 #6:1.2 #7:0.5
2	100	92.9 #3:6.3 #4:0.8	96.33 #3:3.37	94.10 #3:5.9	80.75 #3:19.25	75.50 #3:24.5
3	98.65 #2:1.35	81.40 #2:17.1 #7:1.5	80.70 #1:1.35 #2:3.53 #6:14.43	77.20 #1:1.8 #2:4.6 #5:1.3 #6:15.1	91.80 #2:8.2	86.40 #1:0.5 #2:11.1 #5:0.1 #6:1.8 #7:0.1
4	100	95.80 #5:0.3 #7:3.9	99.95 #7:0.05	97.0 #1:0.6 #2:0.8 #7:1.6	99.98 #6:0.02	96.40 #1:0.2 #5:0.4 #6:2.9 #7:0.1
5	100	93.30 #4:6.7	97.98 #4:2.02	98.70 #4:1.30	100	98.90 #4:1.1
6	100	88.80 #3:9.8 #4:0.3	100	100	100	97.70 #4:2.3
7	100	99.80 #1:0.2	99.70 #4:0.3	97.10 #4:2.9	100	99.55 #1:0.3 #3:0.05 #4:0.1
Overall average	99.83	93.41	96.79	94,91	96.57	93.99

Table 2
Average performance of the classifiers used to classify the vectors built from vibration signals acquired at 1500 rpm in 7 classes. Average calculated over 100 sets of training and testing vectors.

Class	Gaussian		Karhunen-Loève		Neural Network	
	Training	Testing	Training	Testing	Training	Testing
1	100	92.40 #4:2.5 #7:5.1	95.00 #2:2.8 #3:2.2	88.70 #2:6.1 #3:5.1 #5:0.1	93.92 #2:4.15 #7:1.93	90.80 #2:6.5 #5:0.4 #7:2.3
2	100	96.40 #1:3.2 #4:0.4	100	100	99.33 #1:0.67	99.10 #1:0.9
3	100	95.50 #1:3.7 #5:0.8	97.63 #5:2.37	98.30 #5:1.7	100	98.60 #5:1.4
4	100	100	100	100	100	96.50 #1:1.7 #7:1.8
5	100	95.90 #1:1.0 #4:1.9 #7:1.2	96.13 #3:3.87	95.30 #3:4.7	99.60 #1:0.15 #3:0.25	94.30 #1:2.2 #3:3.5
6	100	98.80 #1:1.2	100	100	100	100
7	100	100	100	100	100	99.85 #5:0.05 #6:0.1
Overall average	100	97.38	98.59	97.79	99.10	97.37

Analyzing the classification errors in Table 1, it can be seen that the worst classification error was obtained at the testing stage of neural networks, where 19.15% of training vectors from class 2 (one blade with 1.0 g) were classified as belonging to class 3 (one blade with 1.5 g). This trend was also observed after testing, where 24.5% of the vectors belonging to class 2 were misclassified as belonging to class 3.

The confusion between classes 3 and 2 is also noticeable: here, 17.1% of testing vectors were wrongly classified by the Gaussian discriminator. Significant error levels were also perceived for KLT, where class 3 was confused with class 6 in both training and testing stages with approximately 15% error. The confusion between these two classes also occurred in the testing step of the Gaussian classifier, where 9.8% of vectors belonging to class 6 were misclassified as belonging to class 3. These two classes are characterized by masses of 1.5 g causing the unbalance of the rotor, and therefore both simulate extreme operating conditions which may have caused a greater confusion of classifiers.

It can be seen that the overall averages of the training process (99.83, 96.79, and 96.57%) are higher than those of the testing process (93.41, 94.91, and 93.99%). Again, just as in the classification of vectors derived of vibration signals acquired at 900 rpm [15], this is expected because it is easier to classify data that were supplied to the classifier during the training process.

For class 7, there were some classification errors but not at significant level, supporting the idea that the vibration level of balanced blades is similar to the system without the blades (shaft only).

Even with significant errors, the overall averages of all classifiers were satisfactory, as they were all above 93%, which shows good efficiency in the classification of the signals.

Projecting the vectors along the direction of the eigenvectors (principal components) corresponding to the two largest eigenvalues of the covariance matrix of input vectors generates Fig. 3,

Table 3
Average performance of the classifiers used to classify the vectors built from vibration signals captured at 900, 1200 and 1500 rpm in 21 classes. Results are presented as in Table 1.

Class	Gaussian		Karhunen-Loève		Neural Network	
	Training	Testing	Training	Testing	Training	Testing
1	100	100	100	99.3 #2:0.7	100	99.2 #8:0.1 #14:0.7
2	100	98.4 #4:1.6	100	100	100	99.9 #1:0.1
3	100	99.1 #6:0.9	100	100	100	99.4 #6:0.6
4	100	100	100	100	99.98 #5:0.02	94.7 #5:3.9 #11:1.4
5	100	99.6 #4:0.4	100	100	99.78 #4:0.22	94.2 #4:5.8
6	100	97.7 #4:2.3	95.65 #1:1.9 #2:2.45	94 #1:2.4 #2:3.6	100	99.8 #2:0.1 #3:0.1
7	100	100	100	100	100	99.6 #14:0.3 #18:0.1
8	100	95.8 #10:0.3 #11:1.8 #14:2.1	100	100	99.73 #10:0.27	98.7 #1:0.5 #10:0.3 #11:0.1 #13:0.4
9	100	92.8 #10:6.7 #11:0.5	97.73 #10:2.27	97 #10:3	92.75 #10:7.25	87.4 #10:12.6
10	98.98 #9:1.02	82 #9:16.2 #11:0.1 #14:1.6	73.88 #8:3.28 #9:7.98 #13:14.86	72.3 #8:3 #9:10.3 #13:12.7 #14:1.7	90.55 #3:0.18 #8:0.58 #9:6.53 #11:0.02 #13:0.07 #19:0.25 #21:1.82	86.2 #8:1.0 #9:11.7 #13:0.2 #21:0.9
11	100	97.2 #12:0.1 #14:2.7	96.98 #8:1.58 #9:2.08 #13:2.38	94 #8:2.5 #9:1.8 #13:1.7	98.98 #1:0.1 #8:0.2 #10:0.02 #13:0.7	94.9 #1:0.7 #2:0.1 #4:0.5 #6:0.3 #8:0.2 #9:0.1 #13:2.3 #14:0.7 #21:0.2
12	100	93.1 #11:6.9	99.5 #11:0.5	98.7 #11:1.3	100	99 #9:0.2 #11:0.4 #15:0.3 #19:0.1
13	100	87.6 #10:10.8 #11:0.1 14:1.5	100	100	99.93 #8:0.02 #11:0.05	98.3 #1:0.1 #8:0.9 #11:0.7
14	100	99.75 #1:0.25	98.16 #8:0.05 #11:1.79	97 #8:0.55 #11:2.45	99.98 #11:0.02	99.2 #1:0.3 #11:0.05 #18:0.05 #21:0.4
15	100	92.6 #18:2.9 #21:4.5	95.93 #16:0.18 #17:2.0 #19:1.9	94.6 #16:1 #17:1.9 #19:2.5	94.73 #11: 0.02 #16:3.25 #21:2.0	91.9 #12: 0.7 #16:5.2 #19:0.3 #21:1.9
16	100	95.5 #15:4.1 #18:0.4	92.88 #15:7.12	90 #15:10	98.93 #15:1.07	97.8 #15:2.2
17	100	95.6 #15:3.7 #19:0.7	94.9 #15:2.25 #19:2.85	90.7 #15:4 #19:5.3	99.8 #19:0.2	99.3 #19:0.7
18	100	100	100	99.3 #21:0.7	98.08 #4:0.02 #7:0.25 #11:0.33 #14:1.15 #15:0.02 #21:0.15	89.6 #7:3.8 #11:1.3 #14:1.2 #20:0.1 #21:0.7
19	100		95.98 #17:4.02	96.1 #17:3.9	98.5 #10:0.02	92.7 #15:2.7

(*continued on next page*)

Table 3 (*continued*)

Class	Gaussian		Karhunen-Loève		Neural Network	
	Training	Testing	Training	Testing	Training	Testing
		96.5 #15:1.3 18:1.2 #21:1.0			#15:0.25 #17:1.18 #21:0.05	#17:4.5 #21:0.1
20	100	99.8 #15:0.2	100	100	100	100
21	100	100	100	100	100	99.3 #11:0.05 #15:0.2 #19:0.35 #20:0.1
Overall average	99.96	96.78	97.36	96.67	98.82	96.63

Table 4
Average performance of the classifiers used to classify the vectors derived from vibration signals captured at 900, 1200 and 1500 rpm in 7 classes. Results are presented as in Table 1.

Class	Gaussian		Karhunen-Loève		Neural Network	
	Training	Testing	Training	Testing	Training	Testing
1	90.63 #2:2.29 #3:7.08	88.17 #2:2.77 #3:7.26 #4:1.8	70.80 #2:12.53 #3:7.85 #4:0.13 #5:3.78 #6:4.91	69.83 #2:13.03 #3:7.5 #4:0.23 #5:3.63 #6:5.77	66.66 #2:20.86 #3:4.35 #4:2.44 #5:5.58 #6:0.09 #7:0.02	66.07 #2:19.23 #3:4.7 #4:2.43 #5:6.73 #6:0.07 #7:0.77
2	99.95 #3:0.05	96.87 #1:0.03 #3:2.5 #4:0.6	96.90 #3:1.78 #5:1.32	94.97 #3:2.67 #5:2.37	92.04 #3:7.96	91.63 #1:0.03 #3:8.33
3	97.57 #2:2.43	90.77 #1:0.7 #2:6.9 #4:0.1 #5:0.03 #6:0.97 #7:0.53	64.08 #1:5.79 #2:15.61 #5:0.04 #6:14.48	60.87 #1:5.77 #2:17.1 #5:0.1 #6:16.16	90.18 #1:1.52 #2:3.82 #5:0.07 #6:3.78 #7:0.63	89.77 #1:1.6 #2:4.13 #5:0.13 #6:3.73 #7:0.63
4	100	100	92.88 #1:1.88 #5:1.85 #7:3.38	89.83 #1:2.07 #5:3.4 #7:4.7	96.17 #1:1.21 #3:0.02 #5:1.31 #6:0.7 #7:0.58	93.03 #1:1.53 #3:0.23 #5:2.63 #6:1.13 #7:1.43
5	91.14 #3:8.86	89.37 #1:0.07 #3:8.97 #4:1.6	56.55 #1:4.14 #2:13.07 #3:5.84 #4:1.78 #6:18.62	56.07 #1:4.47 #2:13.7 #3:5.5 #4:2.33 #6:17.93	70.85 #2:0.05 #3:24.24 #4:1.35 #6:2.07 #7:1.43	68.97 #2:0.3 #3:25.27 #4:2.3 #6:1.93 #7:1.23
6	99.18 #3:0.82	95.67 #1:1.0 #2:0.03 #3:3.13 #4:0.17	75.76 #1:0.77 #2:0.65 #3:22.83	72.60 #1:0.8 #2:0.8 #3:25.77 #5:0.03	98.16 #1:0.36 #2:0.3 #3:0.45 #4:0.26 #5:0.35 #7:0.12	97.00 #1:0.47 #2:1.17 #3:0.4 #4:0.3 #5:0.56 #7:0.1
7	100	99.97 #4:0.03	97.03 #1:0.04 #4:2.92 #6:0.01	95.60 #1:0.37 #4:4.03	99.80 #4:0,20	98.73 #1:0.37 #4:0.87 #5:0.03
Overall average	96.92	94.40	79.14	77.11	87,69	86.46

which depicts the results of KLT in classifying vectors obtained at 1200 rpm. It is worth to noting that, because of some high misclassifications, some points on the graph are somewhat overlapped, for example, classes 2 and 3 (red circles and green triangles, respectively) and classes 3 and 6 (green and lilac triangles, respectively), thus illustrating classification errors rates of up to 24%.

Regarding vibration levels that can simulate the working conditions of a wind turbine at high rotations, the analysis procedure was also performed for the rotation speed of 1500 rpm and the results can be seen in Table 2. For almost all training procedures, the results were better than for testing, supporting the fact that it is easier to classify a dataset that was provided to the program during the classification process. The largest errors were also found during

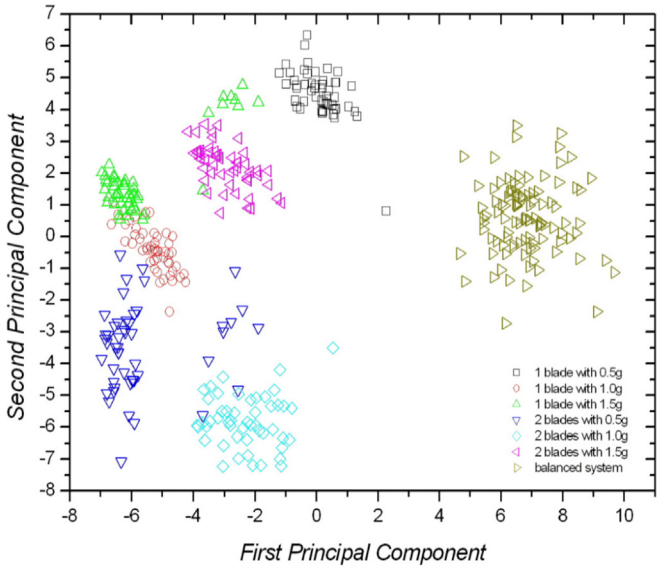

Fig. 3. Karhunen-Loève transformation of the vectors obtained by DFA of signals recorded at 1200 rpm.

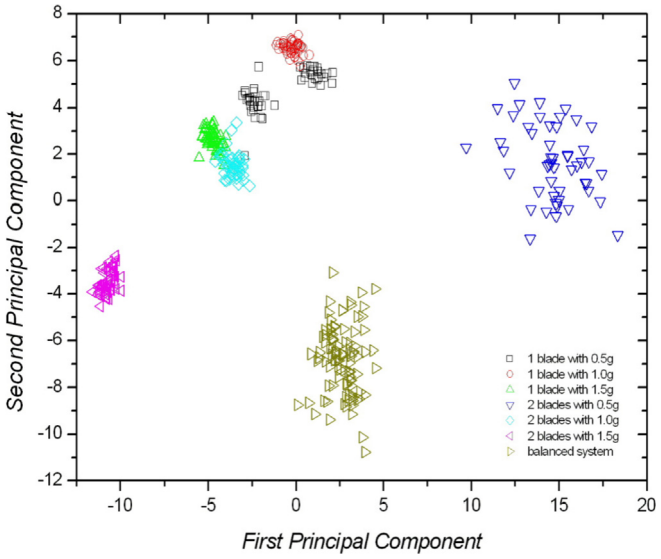

Fig. 4. Karhunen-Loève transformation of the vectors obtained by DFA of signals recorded at 1500 rpm.

the testing stage, where 6.5% of the vectors from class 1 were confused by the neural network with the vectors from class 2. The same confusion was obtained by KLT with a misclassification of 6.1%. However, some misclassifications events were detected at this rotation speed that did not occur in previously evaluated cases; for example, vectors from class 1 were classified as belonging to class 7, reaching 5.1% with the Gaussian classifier. This illustrates that at high rotation speed levels, the vibration level of a small unbalance gets closer to the vibration levels of the system itself, which has a characteristic vibration even when balanced.

Observing class 7, it can be seen that no significant error was identified, once again indicating that the balancing of the system was performed successfully. From these results and despite a blockage ratio of 50.77% and a blockage factor of 0.84, it was observed that there was no change in the vibration measurement procedure and that the classifiers could not distinguish the condition of three balanced blades from the shaft-only case, which approximates to a zero blockage ratio. A similar conclusion can be drawn regarding the surface roughness of the blades.

Fig. 4 depicts the results obtained from application of the KLT classifier to vectors derived from vibration signals acquired at 1500 rpm. Classes 4, 6, and 7 were classified with 100% accuracy as can be noted from the isolated point clusters in the figure. The remaining classes for which small errors were present are represented by very close point clusters, which confuse some data and lead to the classification errors.

In order to compare the vibration levels for each rotation speed tested so far, a new processing was performed using all 1200 collected signals but accounting for all the 21 possible classes, where classes 1 to 7 represent the recorded signals at rotation speed of 900 rpm and introduced by de Moura et al. [15], classes 8 to 14 correspond to the signals from a rotation speed of 1200 rpm, and, classes 15 to 21 are related to 1500 rpm. The seven classes for each rotation speed are the same as the ones for the previous tests. The success rate confusion matrix of this processing round is presented in Table 3.

The overall means for the training step were slightly better than those from the testing step, which was as expected. A correct classification rate of 99.96% was obtained via the Gaussian discriminator for training and 96.78% was obtained for testing, demonstrating the highest efficiency among the classifiers, whereas for ANN and KLT the accuracy rates obtained were 98.82 and 97.36% for the training step and 96.63 and 96.67% for the testing step, respectively. From Table 3, it is clearly understood that all classifiers made it possible to distinguish the cases for each rotation speed even with the occurrence of a few small errors, since the classes for one rotation speed were not confused with the classes for another, which demonstrates that the vibration levels change significantly according to the rotational speed.

The variation in vibration levels is easily observed when the turbine rotation speeds are changed, as can be seen in Fig. 5. Each color represents vectors from a rotational speed and the 21 classes cannot be distinguished due to the two-dimensional character of the figure.

Considering the above aspects and knowing that a wind turbine works at different rotational speeds throughout the day due to the variations in wind intensity, a last step was carried out to simulate a

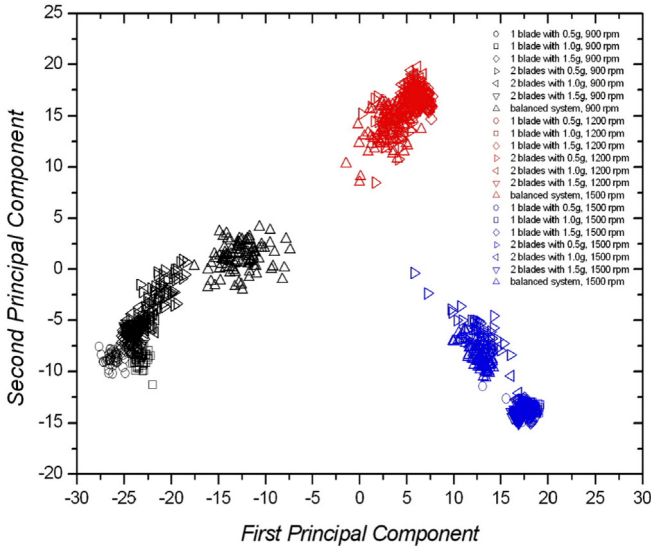

Fig. 5. Karhunen-Loève transformation of the vectors obtained by DFA of signals recorded at the different rotation speeds considered.

wind turbine operating under real conditions, where the same defect (e.g. 0.5 g at the tip of one blade) must be identified at any rotational speed. Thus, the new processing was performed considering all signals captured at the three rotations speed and unlike previous tests, each unbalance level will be represented as a single class regardless of the rotation. Therefore, seven classes will be considered, so that each class represents 150 signals or 50 for each rotation. The results are shown in Table 4.

From these results, it can be seen that the Gaussian discriminator was the most efficient classifier and the second best qualified one was the ANN. For KLT, some difficulties in the classification were found but satisfactory results were generated with overall means above 77%. Some common errors found by employing other analysis scenarios also occurred. There was a high degree of misinterpretation for classes 3 and 6, for example, under KLT; the ANN approach interpreted approximately 25% of the vectors of class 5 as belonging to class 3; both KLT and ANN misinterpreted the vectors of class 1 as belonging to class 2, with errors of approximately 13 and 20%, respectively. Those degrees of confusion were within expectations, since the methods were forcedly applied to classify signals from three different rotation speeds as a single class, which means changing the vibration levels due to the variation of rotational speed.

Despite all the misinterpretations found among the unbalanced classes, vectors from class 7 were classified with a high overall mean correct classification rates – 95.60% was the lowest – which indicates the suitability of all the techniques to differentiate the normal operating condition from those which present any kind of problem. These results show that the techniques may also be applied in alarm systems, indicating the presence of any abnormality in order to proceed with stopping the machine without exactly specifying the failure.

The tests were carried out at three rotational speed levels that represent a wide range of operation of the scaled wind turbine used and can simulate the behavior of the vibration for any rotation speed. In addition, when any type of flaw occurs, regardless of the rotational speed, the techniques employed allow detection of the change in the vibration behavior, indicating the presence of some abnormality.

A performance study of the tested turbine was also carried out, to assess the influence of the wind tunnel's blockage factor, following a similar procedure of Chen & Liou [29]. Accordingly, the maximal Cp (performance coefficient) variations did not reach 10% [30], what is stated as a non disturbed result [29]. This occurs mainly because the blade solidity is small, as is common in real wind turbines. Furthermore, we did not find any signal that Cp and the imbalance levels are related, for all the cases studied.

According to the evaluated cases, there were no changes of imbalance due to the blockage effect that normally occurs in wind tunnels. This was verified by the fact that the algorithms did not change their performance according to the rotation. Given that this effect directly affects the blockage effect, since it grows with the rotation, even without geometric changes in the turbine, the unbalance characteristics should change, which was not verified.

Most techniques traditionally employed for vibration analysis are based on the Fourier transform. For many signals, Fourier analysis is extremely useful because their frequency content is very important. However, Fourier analysis has a serious drawback. After the Fourier transformation, the time information is lost. Therefore, it is impossible to know when a particular event happened by analyzing the Fourier transform of a signal. For steady state time series, this is not a drawback. However, a wind turbine is subject to many sources of vibration, such as meshing gears, shafts, bearings, unbalances, and even wind gusts, and consequently the vibration signals captured from a wind turbine may contain numerous transient or non-stationary characteristics. These characteristics are often the most important part of the signal, and the Fourier analysis is not able to detect them.

In Ref. [9], using a new approach called EDFIL, the vibration signals were decomposed, separating the vibration frequencies of each turbine's component through Fourier transform. Nevertheless, EDFIL does not perform the diagnosis in a simple way, because of the failures present in components which operate under similar rotation velocities and similar vibration frequencies. Besides, with the changes of rotational speed, the classifications of the different crack sizes present in the blades are confused with each other, which makes the results imprecise.

With less computational effort [11], the best-first tree algorithm and the functional trees algorithm presented good results during the classification of six different operating conditions of a wind turbine, with average success rates of 85.33 and 91.67%, respectively. Similar average values were found in the present work with the Neural Network although it had the drawback of a longer processing time.

Among the three classification techniques tested here, the Gaussian discriminator was found to be more adequate for the failure classification, obtaining precise results in all the tests and even presenting the smallest computational cost, thus proving it to be a powerful tool for condition monitoring of wind turbine blades.

6. Conclusion

A first analysis was performed considering constant rotation speeds and seven work conditions. DFA combined with pattern recognition techniques proved to be effective in identifying the imbalance levels studied. At 900 rpm, all classifiers achieved satisfactory results. The lowest success rate among them was obtained by ANN, with a 99.96% success rate in the classification of training data and 98.67% during testing. The best results were obtained by application of KLT. The success rate reached 100 and 99.88% for the training and testing data, respectively, followed by the Gaussian discriminator at 100 and 99.31%. At 1200 rpm, the misclassification rate was slightly higher than obtained at 900 rpm. The lowest average success rate was 93.41% in the test step with the Gaussian classifier. The success rates reached 93.99 and 94.91% in the test step with ANN and KLT, respectively. Despite this, the Gaussian discriminator achieved the best success rate in the training step, with 99.83% of vectors being correctly classified compared to 96.79% and 96.57% for KLT and ANN. In the tests at the highest rotational speed (1500 rpm), similar results were obtained by all the classifiers: 100% of training data were correctly classified by the Gaussian discriminator and the best test performance (97.79%) was reached by the KLT.

When the training procedure of the classifiers was done under 21 work conditions obtained by a combination of seven imbalance levels and three rotational speeds, it was found that the vibration levels changed considerably as the blades' velocity changed. Despite this, the classifiers presented good performances with average success rates above 96% in all cases, even with a larger number of classes involved.

In the last simulation round, seven classes were considered, one for each imbalance level independently of the rotational speed. This is closer to the actual operating conditions; that is, the defects must be identified at any rotation speed. More strict conditions were faced and more difficulties became evident. For KLT, for example, although an overall average of 77.11% was obtained in the test step, a success rate of only 56.07% was achieved in the classification of the class 5 vectors. However, the Gaussian discriminator correctly classified 94.40% of vectors during testing, an excellent performance even though this classifier had the least computational cost.

The ANN was able to classify the test signals according to their imbalance levels with a success rate in excess of 86.46%, which is a reasonable and satisfactory result.

In spite of all the classification errors found at the three rotation speeds tested, the balanced class was always well separated, indicating that the classifiers are able to distinguish the normal functioning condition from those with some abnormality. Moreover, in most cases, the different unbalance levels were indicated with high precision, also demonstrating that this approach is a powerful tool for predictive maintenance.

Another important observation is the small difference between the overall mean rates of correct classification achieved on training and testing data. This provides a confirmation of the suitability of the classifiers studied in identifying unknown signals that are key for the detection of defects that may arise at the blades of a wind turbine.

In general, the results showed that the approach applied in this work may be useful for the development of monitoring systems based on vibration analysis of wind turbine blades. As an important part of predictive maintenance, automatic vibration analysis of a wind turbine could save a lot of resources due to unnecessary stoppages and labor costs.

Acknowledgements

This study was financed in part by the Coordenação de Aperfeiçoamento de Pessoal de Nível Superior - Brasil (CAPES) - Finance Code 001. We also gratefully acknowledge the financial support of the Brazilian agencies CNPq and FUNCAP.

References

[1] Blanco MI. The economics of wind energy. Renew Sustain Energy Rev 2009;13:1372–82.
[2] Sareen A, Sapre CA, Selig MS. Effects of leading edge erosion on wind turbine blade performance. Wind Energy 2014;17:1531–42.
[3] Dalili N, Edrisy A, Carriveau R. A review of surface engineering issues critical to wind turbine performance. Renew Sustain Energy Rev 2009;13:428–38.
[4] Yang B, Sun D. Testing, inspecting and monitoring technologies for wind turbine blades: a survey. Renew Sustain Energy Rev 2013;22:515–26.
[5] Sagol E, Reggio M, Ilinca A. Issues concerning roughness on wind turbine blades. Renew Sustain Energy Rev 2013;23:514–25.
[6] Soltani MR, Birjandi AH, Moorani MS. Effect of surface contamination on the performance of a section of a wind turbine blade. Sci Iran 2011;18:349–57.
[7] Yokoyama S. Lightning protection of wind turbine blades. Electr Power Syst Res 2013;94:3–9.
[8] Moura Carneiro FO, Barbosa Rocha HH, Costa Rocha PA. Investigation of possible societal risk associated with wind power generation systems. Renew Sustain Energy Rev 2013;19:30–6.
[9] Abouhnik A, Albarbar A. Wind turbine blades condition assessment based on vibration measurements and the level of an empirically decomposed feature. Energy Convers Manag 2012;64:606–13.
[10] Liu WY, Zhang WH, Han JG, Wang GF. A new wind turbine fault diagnosis method based on the local mean decomposition. Renew Energy 2012;48:411–5.
[11] Joshuva A, Sugumaran V. A data driven approach for condition monitoring of wind turbine blade using vibration signals through best-first tree algorithm and functional trees algorithm: a comparative study. ISA Trans 2017;67:160–72.
[12] Pérez JS, Arredondo MAT, Güemes A. Damage and nonlinearities detection in wind turbine blades based on strain field pattern recognition. FBGs, OBR and strain gauges comparison. Compos Struct 2016;135:156–66.
[13] Peng CK, Buldyrev SV, Havlin S, Simons M, Stanley HE, Goldberger AL. Mosaic organization of DNA nucleotides. Phys Rev 1994;49:1685–9.
[14] de Moura E, Souto C, Silva A, Irmão M. Evaluation of principal component analysis and neural network performance for bearing fault diagnosis from vibration signal processed by RS and DF analyses. Mech Syst Signal Process 2011;25:1765–72.
[15] de Moura E, Melo Junior FEA, Damasceno FF, Figueiredo LCC, Andrade CF, Almeida MS, Rocha PA. Classification of imbalance levels in a scaled wind turbine through detrended fluctuation analysis of vibration signals. Renew Energy 2016;96:993–1002.
[16] de Almeida MS. Computational design of blades for horizontal-axis wind turbine (in Portuguese). Master's thesis. Universidade Federal do Ceará; 2013.
[17] Burton T, Sharpe D, Jenkins N, Bossanyi E. Wind energy handbook. John Wiley & Sons; 2001.
[18] Podobnik B, Stanley HE. Detrended cross-correlation analysis: a new method for analyzing two non-stationary time series. Phys Rev Lett 2008;100:084–102.
[19] de Moura E, Vieira A, Irmão M, Silva A. Applications of detrended-fluctuation analysis to gearbox fault diagnosis. Mech Syst Signal Process 2009;23:682–9.
[20] Matos JMO, de Moura E, Krüger SE, Rebello JMA. Rescaled range analysis and detrended fluctuation analysis study of cast irons ultrasonic backscattered signals. Chaos, Solitons Fractals 2004;19:55–60.
[21] de Moura E, Normando P, Gonçalves L, Kruger S. Characterization of cast iron microstructure through fluctuation and fractal analyses of ultrasonic backscattered signals combined with classification techniques. J Nondestr Eval 2012;31:90–8.
[22] Vieira A, de Moura E, Gonalves L, Rebello J. Characterization of welding defects by fractal analysis of ultrasonic signals. Chaos, Solit Fractals 2008;38:748–54.
[23] Schlechtingen M, Santos IF. Comparative analysis of neural network and regression based condition monitoring approaches for wind turbine fault detection. Mech Syst Signal Process 2011;25:1849–75.
[24] Odgaard PF, Stoustrup J. Karhunen Loeve basis used for detection of gearbox faults in a wind turbine. IFAC Proc 2014;47:8891–6.
[25] Valencia LDA, Fassois SD. Damage/fault diagnosis in an operating wind turbine under uncertainty via a vibration response Gaussian mixture random coefficient model based framework. Mech Syst Signal Process 2017;91:326–53.
[26] Haykin S. Neural networks: a comprehensive foundation. International edition. Prentice Hall; 1999.
[27] Wasserman P. Neural computing: theory and practice. A Van Nostrand Reinhold Book, Van Nostrand Reinhold; 1989.
[28] Webb AR. Statistical pattern recognition. second ed. John Wiley & Sons; 2002.
[29] Chen TY, Liou LR. Blockage corrections in wind tunnel tests of small horizontal-axis wind turbines. Exp Therm Fluid Sci 2011;35.
[30] Diniz MAB. Aerodynamic performance of a scale wind turbine, Profile NREL S809, with different specific design speeds. Brazil: Master Thesis, Department of Mechanical Engineering of Federal University of Ceará; 2014 [In Portuguese].